Vol. 43, No. 4 (2021) 535-542, DOI: 10.24874/ti.1015.11.20.05

Tribology in Industry

www.tribology.rs

RESEARCH

Instrumented Scratch Testing of Metal Coatings Produced by Screen Printing (SP) and Aerosol Deposition (AD) Technology

N. Laszlo[a,*]

[a]*Bay Zoltan Nonprofit Ltd. for Applied Research, Igloi ut 2. Miskolc, H-3519 Hungary.*

Keywords:

$BaTiO_3$
Screen printing
Aerosol deposition
Coating
Scratch
Friction

* Corresponding author:

Noemi Laszlo
E-mail: noemi.laszlo@bayzoltan.hu

Received: 30 November 2020
Revised: 24 December 2020
Accepted: 5 May 2021

A B S T R A C T

Screen printing (SD) is a simple and well-developed coating technology widely used today, but it is time consuming, expensive, and not environmentally friendly due to the organic solvents used in the technology. The aerosol deposition (AD) coating process can be an alternative to this method, due to the homogeneous properties (e.g. density, roughness, etc.) and environmental friendliness of the deposited coatings. This paper presents the results of a comparative mechanical tribological study of metal coatings (Cu, Al) deposited on a ceramic substrate ($BaTiO_3$) by screen printing and aerosol deposition technology. To compare the coating technologies, we examined the tribological behavior of coatings and the damage mechanism by instrumental scratch test.

1. INTRODUCTION

The production of ceramic components usually requires temperatures above 900-1000 °C due to sintering processes, which can be especially problematic for electronic components [1,2], where integration with metals or even plastics may often be required [3]. For the most used technologies for coating electronic components [4], such as CVD, screen printing, etc. the temperature requirement of the process is associated with significant cost implications. However, not all technologies can be used for individual electronic applications, an example of which is shown in Fig. 1, which compares the technologies that can be applied to each electronic component based on the characteristics of the coatings [5,6].

Screen printing (SP) is a printing technology [7-11] that uses systems made of metallic and non-metallic fibers (so-called screen fabrics). As one type of screen printing, screen printing involves passing ink through a fine mesh of screen printing by pressing a rubber insert or other means in order to print the ink on the target (substrate). The method can be used to coat samples of any surface (flat, uneven and

curved) and materials. SP technology can also be used for multilayer ceramic capacitors (MLCCs), where the basic goal is to maximize performance while reducing dimensions. Aerosol deposition coating process can be considered as a novel technology for separating metallic and non-metallic, thin, and thick coatings by spraying solid powder. Its advantages over screen printing technology are room temperature processing, mass production capability and relatively inexpensive technology [5].

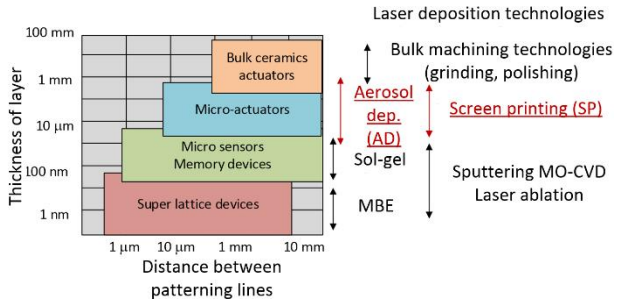

Fig. 1. Comparison of fabrication methods in case of electronic components [3].

Although SP is a frequently used technology for MLCCs and LTCC [8,9] components, there is a growing need to develop and apply lower temperature, more environmentally friendly technologies. A suitable alternative is aerosol deposition (AD) technology [12-14], which can produce even more uniform layer thickness and more homogeneous coatings.

Referring to
Fig. **2** [12], schematic diagram illustrating AD technology is shown. The process can be described as follows [15]:

1) Generate a powder aerosol, transport by a pressure difference to a vacuum chamber.
2) Acceleration of the aerosol to 100 m/s by means of a nozzle
3) In contact with the substrate surface of the aerosol, film formation.

In the case of AD technology, a number of studies have examined the mechanisms [16-19] required for layer formation, and the formation of the film can best be illustrated with the help of Fig. 3. It is assumed that stratification can be described as follows: the submicrometer particles of the coating impinge on the substrate material at high kinetic energy, causing them to shatter and form nanometer-sized debris. The debris is constantly compacted, deposited because of new colliding particles. The thickness of the layer can be controlled by the deposition time.

The thickness of the resulting coating is around 1-300 µm, it has good adhesion properties, mechanical and thermal stability, which is comparable to the base material of the powder [20-23].

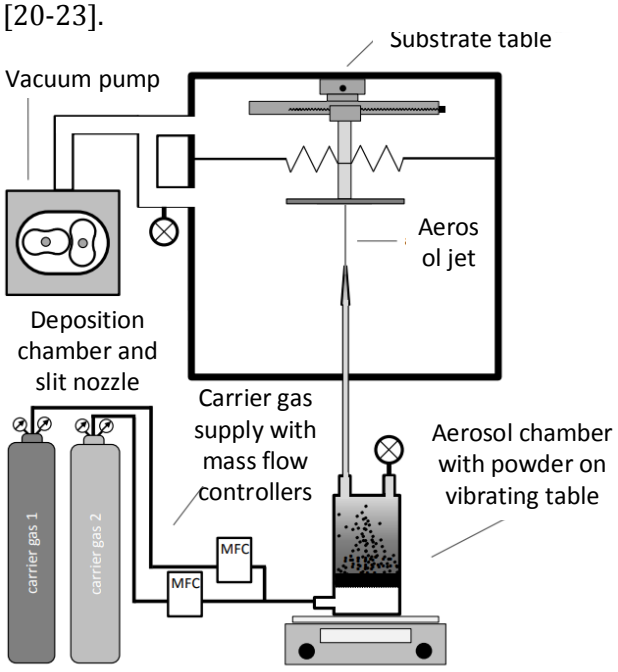

Fig. 2. Schematic drawing of AD device [12].

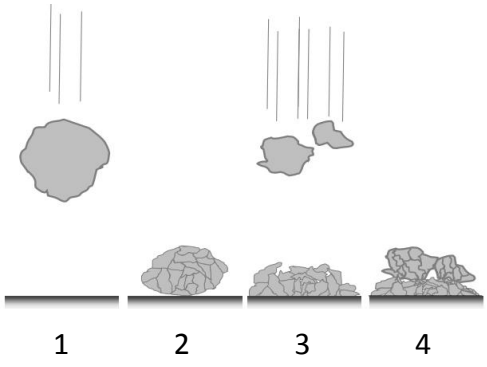

Fig. 3. Mechanism of film formation in case of AD technology [12].

Accurate knowledge of the adhesion behavior of coatings is important, as improper adhesion can cause damage to the coating (e.g., chipping, delamination, etc.) and thus product failure. For this reason, the adhesion properties of the coatings were characterized by instrumented

scratch testing. The purpose of scratch testing has traditionally been to examine the adhesion and damage [24-33] of hard coatings [34-40], but there is a growing need to extend the test to determine the scratch resistance of other types of coated systems, surface-treated gradient surface structures [41-44] or monolithic materials [45-48].

2. METHODS

In our investigations, we examined aluminum and copper coatings deposited on $BaTiO_3$ ceramic substrates by screen printing (SP) and aerosol deposition technology (AD).

In case of AD technology, Cu and Al powder with an average particle size of 2 μm and 3-5 μm was mixed with a carrier gas with a flow rate of 10 l/min. The granular mixture of the carrier gas-metal particle thus formed was aerosolized in an aerosol chamber. The gas pressure was 0.2 MPa. The thickness and the surface roughness (R_q) of different coatings is shown in Table 1. The layer thickess of AD_Al coatings is 5.3-5.5 mm, the AD_Cu layer is thinner, 1 μm. In the case of the Al layer deposited by screen printing, the layer thickness is 8.1 μm and the value of R_q is 1.2 μm.

Table 1. The thickness and surface roughness of AD and SP coatings.

	HV0.01			
	AD_Al	AD_Al_p	AD_Cu	SP_Al
Thickness, μm	5,5	5,3	1,0	8,1
R_q, μm	1,2	0,9	1,1	1,2

The characteristics of the tested samples are shown in Table 2. The tested samples are illustrated by Fig. 4.

Table 2. Characteristics of coatings.

Parameter	HV0.01			
	SP_Al	AD_Al	AD_Al_p	AD_Cu
Substrate	$BaTiO_3$			
Surface prep.	-	rough grinding	fine grinding	rough grinding
Coating	Al			Cu
Coating color	dark grey	fine grey		burgundy

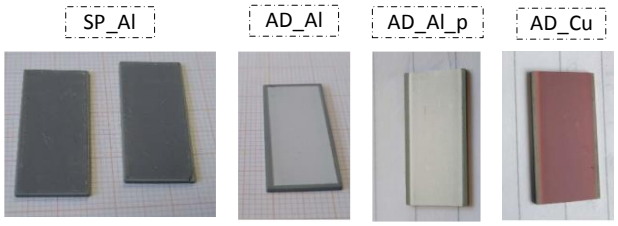

Fig. 4. Screen printed and aerosol deposited coating layers on $BaTiO_3$ samples.

In the case of the SP-Al reference sample, SEM analysis was also performed on the cross-sectional grinding, which is illustrated in the Fig. 5.

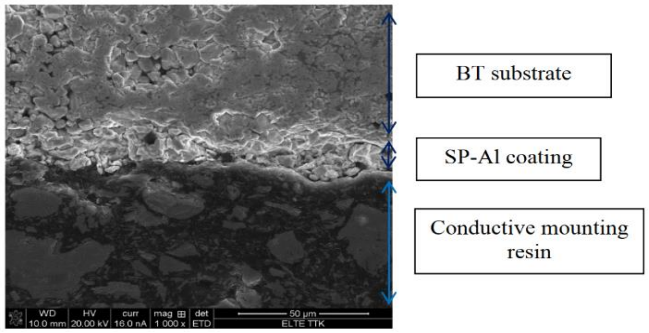

Fig. 5. SEM image of BT ceramic substrate and SP–Al coating (metallographically prepared cross section)

Studying Fig. 5, it can be observed that the BT ceramic substrate is highly porous indicating that the amount of sintering additives was not enough or the temperature was too low during the reaction sintering process.

3. RESULTS

3.1 Microhardness test

Microhardness of base material and coatings was performed with a Mitutoyo MicroVickers hardness tester, which can be used with a loading force of F = 0.1–10 N (Table 3. and
Fig. 6.). The selected loading force was F = 0.1 N, the load duration was t = 10 s.

Table 3. Results of microVickers hardness tests of BT base material (HV0.01, F = 0.1 N, t = 10 s).

Sample	HV0.01		
	Average	Std. dev.	Std. dev [%]
SP_Al (ref.)	263	4.618	1.8
AD_Al	277	9.018	3.3
AD_Al_p	269	9.018	3.4
AD_Cu	278	23.065	8.3

Measurements were performed on each surface quality and the average of the obtained results was used as a basis. In case of base material, the hardness was determined on the cross-sectional grinding, while in the case of the coatings, the surface hardness was measured.

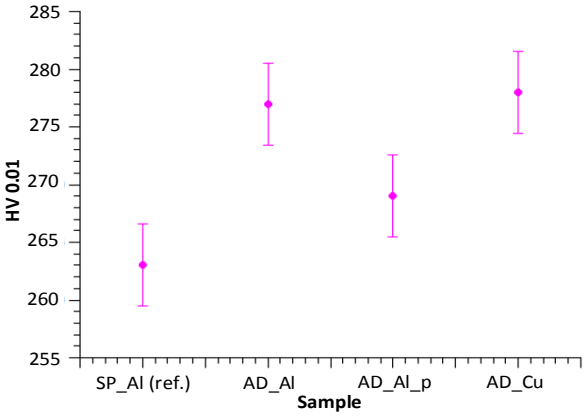

Fig. 6. HV0.01 microVickers hardness of the BT base material by the different samples.

The results show that the layers deposited with aerosol deposition technology have a higher hardness compared to the reference screen printing coating. Under the present experimental conditions, an average hardness increase of about 4-5% is observed, in the case of surfaces prepared by polishing, this value is smaller.

3.2 Instrumented scratch test

Adhesion is an important feature of different coatings, which is why the first step is to quantify some adhesion characteristics. In this case: the critical load required to detach the coating. An instrumental scratch test was used to determine this coating parameter. The scratch tests were performed using an SP-15 scratch tester. The tests were performed with increasing load, the load force applied during the tests was 2-70 N, and the F_{grad} value was 10 N/mm.

The tests were performed with increasing loading force and were first performed on the Cu-coated sample that was assumed to withstand the highest load. A loading force of 100 N was used in the preliminary experiments; however, reaching the 70 N loads was caused by an unexpected break of the specimen (this phenomenon was also observed later). Fig. 7 illustrates the characteristic diagram obtained in the case of scratch tests performed on the AD_Cu sample.

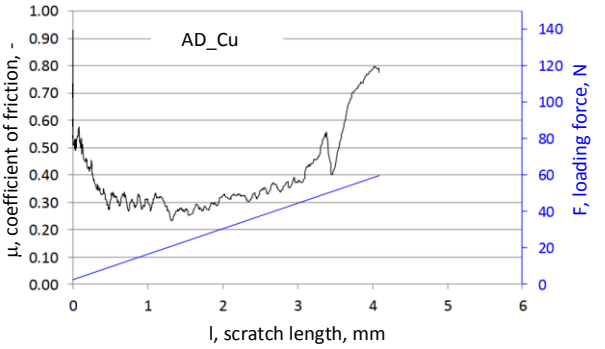

Fig. 7. Scratch diagrams determined during examination of sample AD_Cu.

At loads $F_{c,t}$= 60 N and higher, the formation in the substrate is unfavorable load condition can cause the ceramic substrate to crack or break. On the fracture line of the samples under relatively small loads in the case of the disintegrated pieces, during the visual inspection of the substrate, the breaking of thin, sharp, paddle-like pieces was observed, due to the fact that the $BaTiO_3$ ceramic, which serves as the support material, has significant porosity and stress-collecting material continuity deficiencies. The phenomenon clearly indicates the coating is plastic and carrier for the brittle behavior of ceramics. It also follows that, on the one hand, in the case of the investigated coating system, it does not make sense to look for the critical force associated with the release of the coating, and on the other hand, the critical load ($F_{c,bk}$) causes damage or the destruction of the examined material system - substrate + coating - ($F_{c,t}$), which in the examined case is the fracture of the substrate ceramic.

Damage to a plastic coating formed on such a brittle substrate typically occurs by a different mechanism than in the case of classical hard-coated systems, where the load causing cracking and chipping of the brittle, high-hardness coating on the metallic substrate is sought. Nevertheless, the study may provide a wealth of information on the behavior of such coating systems.

Based on the performed tests, it can be stated that the presence of the coating provides favorable frictional conditions up to a load in the direction of F = 20-30 N, i.e. with a slight increase in the load force the value of the coefficient of friction is μ=0.5-0.6. sliding friction after the state is set, it decreases to a value around μ=0.25. This behavior was observed in all cases examined until the given load was reached, regardless of the scratch path length (L)

and the maximum load force (F_{max}). In the load range $F_{c,\,bk}$ = 30-50 N, the degree of damage to the coating - presumably due to peeling due to plastic deformation - increases monotonically with the value of the coefficient of friction.

In the case of the AD_Al samples discussed above, the surface of the ceramic substrate was coarsely sanded prior to coating, while in the case of the AD_Al_p samples, the ceramic surface under the coating was polished, i.e. the examined metal layer was placed on the surface. Based on the scratch tests performed on the AD_Al_p sample (Fig. 8), it can be observed that the behavior of the polished samples before coating is very similar to the scratch test of the same coating applied to coarsely ground ceramic substrate, when increasing the value of F_{max}. The behavior is also similar in that the value of the coefficient of friction decreases monotonically during the (increasing load) test and the threshold value of the load force – $F_{c,s}$≈40 N – at which the coefficient of friction μ≈0.25 is determined by analyzing the six diagrams stabilizes around. Thus, compared to a similar coating made with a coarsely ground substrate, the coating applied to the polished substrate is characterized by a slightly higher $F_{c,s}$ load force and the associated constant coefficient of friction.

From the scratch tests performed on the reference sample, it can be seen, that the scratch behavior of the sample with respect to scratch diagrams is very similar to that of samples AD_Al and AD_AL_p. The local maximum of the coefficient of friction seen at the beginning of the test occurred only at the first scratching of this sample, which confirms the assumption that the compaction and adhesion of the new technology coatings to the tool may be the cause of the phenomenon.

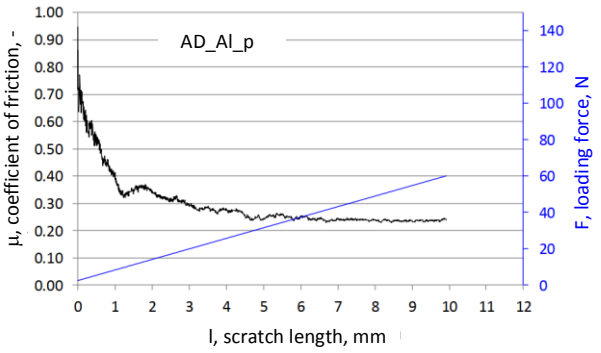

Fig. 8. Scratch diagrams determined during examination of sample AD_Al_p.

For the reference sample SP_Al, the scratch diagram is illustrated in the Fig. 9.

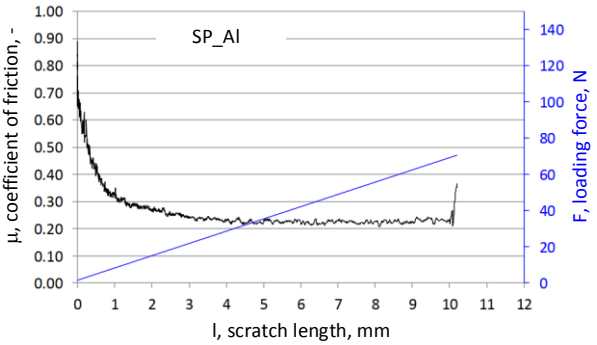

Fig. 9. Scratch diagrams determined during examination of sample SP_Al.

The formation of a constant value of the coefficient of friction can also be observed here, which occurs at normal loads higher than the threshold load $F_{c,s}$=40 N, its value μ=0.22. The Critical load causing the ceramic substrate to break is $F_{c,t}$ ≈70 N. The results presented above are summarized in 4.

Table 4. Results of scratch tests on coatings deposited with SP and AD technology.

Sample	Results of instrumented scratch test		
	$F_{c,s}$, N	$F_{c,t}$, N	μ, –
SP_Al (ref.)	40	70	0.22
AD_Al	30	60	0.2
AD_Al_p	40	60	0.25
AD_Cu	30-50	60	0,25

Based on the table, it can be concluded that the 4 coating systems show similarities in terms of behavior. In the case of aluminum coatings, all three samples (SP_Al, AD_Al and AD_Al_p) are characterized by the stabilization of the coefficient of friction during the scratch test. The value of the corresponding force $F_{c,s}$ is almost similar. In the case of the coarsely polished sample AD_Al, 30 N is the value of the other two samples, i.e. in the case of the sample AD_Al_p (polished) and SP_Al. The value of the steady-state coefficient of friction is μ=0.2, respectively; 0.25 and 0.22, so they are practically the same value. Overall, it can be concluded that in all cases the scratch test was accompanied by a breakage of $BaTiO_3$ ceramic base material, which occurred at a loading force of 60 N.

4. CONCLUSION

In the present paper, we investigated the tribological behaviour of metallic coatings applied to ceramic substrates using different coating technologies. Based on the performed tests, the following conclusions can be made:

1. In the case of aerosol deposition technology there is a slight increase in hardness compared to the coating deposited with screen printig technology, in case of thinner layer thickness. In the case of surfaces prepared by polishing, the hardening-increasing effect is less noticeable.
2. Among the investigated coating systems, the scratching behaviour of the Cu-coated sample is fundamentally different from that of the other three, i.e. Al-coated samples. The obtained scratch diagrams indicate early (low load) damage to the coating, and no condition characterized by a constant coefficient of friction develops during scratching. Overall, this coating system is least stressed during scratch testing.
3. With the exception of the Cu coating, no load can be determined on the test specimens that cause critical damage or detachment of the coating without damaging or breaking the ceramic substrate. In the case of AD_Cu samples, in the loading force range $F_{c,s}$=30-40 N, the increase in the coefficient of friction on the scratch diagrams indicates the onset of damage to the coating, and further investigations are needed to map this.
4. It is made with two types of technology or different for one technology Al - coated samples applied after surface treatment - coarse sanding, polishing its behaviour during scratching is very similar.
5. It is somewhat different that in the initial section of the scratch diagrams of the Al-coated samples applied with the new technology, a local maximum appears systematically in the value of the coefficient of friction, while this phenomenon can be detected only in the first examination of the Al-coated sample with the traditional technology.
6. For all four types of samples, the critical load ($F_{c,t}$) that causes the load capacity limit of the ceramic substrate, i.e., fracture, can be determined. This critical load is 60 N for the new type of sample and 70 N for the reference sample.
7. Under the present test conditions, fracture of the $BaTiO_3$ ceramic substrate was observed, which can be explained by the high porosity resulting from the production of the raw material. At the same time, it can also be said that the raw material is destroyed sooner compared to the coating.

REFERENCES

[1] P. Muralt, A. Kholkin, M. Kohli, T. Maeder, K.G. Brooks, R. Luthier, *Fabrication and Characterization of PZT Thin Films for Micromotors*, Integrated Ferroelectrics, vol. 11, iss. 1-4, pp. 213-220, 1995, doi: 10.1080/10584589508013593

[2] M. Tabib-Azar, Electrical Microactuators, in M. Tabib-Azar (Ed.): Microactuators: Electrical, Magnetic, Thermal, Optical, Mechanical, Chemical and Smart Structures, Springer, pp. 37-94, 1998, ISSN 1386-3290 doi: 10.1007/978-1-4615-5445-5

[3] J. Akedo, *Room Temperature Impact Consolidation (RTIC) of Fine Ceramic Powder by Aerosol Deposition Method and Applications to Microdevices*, Journal of Thermal Spray Technology, vol. 17, iss. 2, pp. 181-198, 2008, doi: 10.1007/s11666-008-9163-7

[4] M.G. Say, R. Brooke, J. Edberg, A. Grimoldi, D. Belaineh, I. Engquist, M. Berggren, *Spray-coated paper supercapacitors*, npj Flexible Electronics, vol. 4, no. 14, pp. 1-7, 2020, doi: 10.1038/s41528-020-0079-8

[5] C C. Lee, M.-Y. Cho, M. Kim, J. Jang, Y. Oh, K. Oh, S. Kim, B. Park, B. Kim, S.-M. Koo, J.-M. Oh, D. Lee, *Applicability of Aerosol Deposition Process for flexible electronic device and determining the Film Formation Mechanism with Cushioning Effects*, Scientific Reports, vol. 9, pp. 1-10, 2019, doi: 10.1038/s41598-019-38477-y

[6] H.D. Chen, K.R. Udayakumar, C.J. Gaskey, L.E. Cross, J.J. Bernstein, L.C. Niles, *Fabrication and Electrical Properties of Lead Zirconate Titanate Thick Films*, Journal of American Ceramic Society, vol. 79, iss. 8, pp 2189-2192, 1996, doi: 10.1111/j.1151-2916.1996.tb08957.x

[7] Shaping the Feature of Automation, Screen Printing, https://www.keyence.com/ss/products/measure/sealing/coater-type/screen-printing.jsp, accessed: 28.11.2020

[8] K. Grennan, A.J. Killard, M.R. Smyth, *Physical Characterizations of a Screen-Printed Electrode for Use*

in an Amperometric Biosensor System, Electroanalysis, vol. 13, iss. 8-9, pp. 745-751, 2001, doi: 10.1002/1521-4109(200105)13:8/9%3C745::AID-ELAN745%3E3.0.CO;2-B

[9] M.R. Somalu, A. Muchtar, W.R.W. Daud, N.P. Brandon, *Screen-printing inks for the fabrication of solid oxide fuel cell films: A review*, Renewable and Sustainable Energy Reviews, vol. 75, pp 426-439, 2017, https://doi.org/10.1016/j.rser.2016.11.008

[10] M. Tudorache, C. Bala, *Biosensors based on screen-printing technology, and their applications in environmental and food analysis*, Analytical and Bioanalytical Chemistry volume, vol. 388, no. 3, pp. 565-578, 2007, doi: 10.1007/s00216-007-1293-0

[11] M. Ihle, U. Partshc, S. Mosch, A. Goldberg, *Aerosol Printing of High-Resolution Films for LTCC-Multilayer Components*, Journal of Microelectronics and Electronic Packaging, vol. 9, no. 3, pp. 133-137. 2012, doi: 10.4071/imaps.340

[12] D. Schwanke, J. Pohlner, A. Wonisch, T. Kraft, J. Geng, *Enhancement of Fine Line Print Resolution due to Coating of Screen Fabrics*, Journal of Microelectronics and Electronic Packaging, vol. 6, iss. 1, pp. 13–19, 2009, doi: 10.4071/1551-4897-6.1.13

[13] Y. Imanaka, N. Hayashi, M. Takenouchi, J. Akedo, *Aerosol deposition for post-LTCC, Journal of the European Ceramic Society*, vol. 27, iss. 8–9, pp. 2789-2795, 2007, doi: 10.1016/j.jeurceramsoc.2006.11.055.

[14] D. Hanft, J. Exner, M. Schubert, T. Stöcker, P. Fuierer, R. Moos, *An Overview of the Aerosol Deposition Method: Process Fundamentals and New Trends in Materials Applications*, Journal of Ceramic Science and Technology, vol. 6, no. 3, pp. 147-182, 2015, doi: 10.4416/JCST2015-00018

[15] Dense ceramic coatings manufactured with the Aerosol-Deposition Method (ADM) at the Department of Functional Materials, http://www.funktionsmaterialien.de/docs/Highlight_ADM_ENG.pdf, accessed: 29. 11. 2020

[16] R. Inada, K. Okuno, S. Kito, T. Tojo, Y. Sakurai, *Properties of Lithium Trivanadate Film Electrodes Formed on Garnet-Type Oxide Solid Electrolyte by Aerosol Deposition*, Materials, vol. 11, iss. 9, pp. 1570, pp.1-13., 2018, doi: 10.3390/ma11091570

[17] M. Schubert, C. Münch, S. Schuurman, V. Poulain, J. Kita, R. Moos, *Thermal Treatment of Aerosol Deposited $NiMn_2O_4$ NTC Thermistors for Improved Aging Stability*, Sensors, vol. 18, iss. 11, pp. 1-16, 2018, doi: 10.3390/s18113982

[18] J. Akedo, J. Ryu, J. Ryu, D.-Y. Jeong, S.D. Johnson, J. Akedo, *Aerosol Deposition (AD) and Its Applications for Piezoelectric Devices*, Advanced Piezoelectric Materials (Second Edition), Science and Technology, pp. 576-614, 2007, doi: 10.1016/B978-0-08-102135-4.00015-1

[19] D. Hanft, P. Glosse , S. Denneler, T. Berthold, M. Oomen, S. Kauffmann-Weiss, F. Weis, W. Häßler , B. Holzapfel, R. Moos, *The Aerosol Deposition Method: A Modified Aerosol Generation Unit to Improve Coating Quality*, Materials, vol. 11, iss. 9, pp. 1-11, 2018, doi: 10.3390/ma11091572

[20] D.-W. Lee, O.-Y. Kwon, W.-J. Cho, J.-K. Song, Y.-N. Kim, *Characteristics and mechanism of Cu films fabricated at room temperature by aerosol deposition*, Nanoscale Research Letters, vol. 11, pp. 1-8, 2016, doi:10.1186/s11671-016-1378-9

[21] M.-Y. Cho, D.-W. Lee, P.-J. Ko, S.-M. Koo, J. Kim, Y.-K. Choi, J.-M. Oh, *Adhesive mechanism of Al_2O_3/Cu composite film via aerosol deposition process for application of film resistor*, Electronic Materials Letters, vol. 15, iss. 2, pp. 227-237, 2019, doi: 10.1007/s13391-018-00111-w

[22] M. Nakada, T. Kawasaki, M.Iwanawi, K. Ohashi, *Application of Electronic Devices for Aerosol Deposition Methods, Functional Element*, Nec Technical Journal, vol. 2, no. 1, pp. 76-80, 2007.

[23] J. Akedo, M. Lebedev, *Microstructure and Electrical Properties of Lead Zirconate Titanate ($Pb(Zr52/Ti48)O_3$) Thick Films Deposited by Aerosol Deposition Method*, Japanese Journal of Applied Physics, vol. 38, no. 9S, pp. 5397–5401, 1999, doi: 10.1143/jjap.38.5397

[24] F. Fülöp, M.B. Maros, *Scratch damage mechanism transition maps of DLC coated cold work tool steels using instrumented scratch test and fractography*, in Fractography of advanced ceramics VI, 8-11 September, 2019, Smolenice, Slovak Republic, Institute of Materials Research, Slovak Academy of Sciences, doi: 10.13140/RG.2.2.26681.11362

[25] S.R.A. Siddiqui, A.S. Biró, M.B. Maros, *Characterization of Scratching Behaviour of Surface Layers Produced on X42cr13 Plastic Mould Tool Steel By Duplex Heat Treatment*, in: Doctoral Forum, University of Miskolc, 2017, pp. 97-104, 2017.

[26] A.O. Sergici, N.X. Randall, *Scratch testing of coatings*, Advanced Materials and Processes, vol. 164, iss. 4, pp. 41-43, 2006.

[27] ISO 27307:2015, *Thermal spraying - Evaluation of adhesion/cohesion of thermal sprayed ceramic coatings by transverse scratch testing*, 2015.

[28] Characterization of thermal spray coatings by Instrumented Indentation and Scratch Testing (Part I), https://www.anton-paar.com/corp-en/products/applications/characterization-of-thermal-spray-coatings-by-instrumented-indentation-and-scratch-testing-part-i/, accessed: 29. 11. 2020.

[29] A.J. Perry, *Scratch adhesion testing of hard coatings*, Thin Solid Films, vol. 107, iss. 2, pp. 167-180, 1983, doi: 10.1016/0040-6090(83)90019-6

[30] S.J. Bull, D.S. Rickerby, A. Matthews, A.R. Pace, A. Leyland, *Scratch Adhesion Testing of Hard, Wear Resistant Coatings*, Plasma Surface Engineering, vol. 1&2, pp. 1227-1234, 1989

[31] P.A. Steinmann, Y. Tardy, H.E. Hintermann, *Adhesion testing by the scratch method: The influence of intrinsic and extrinsic parameters on the critical load*, Thin Solid Films, vol. 154, iss. 1-2, pp. 333-349, 1987, doi: 10.1016/0040-6090(87)90377-4

[32] L. Duanjie, *Understanding Coating failures using scratch testing*, http://servidor.demec.ufpr.br/disciplinas/EME715/Normas%20AT/Ensaio%20Riscamento/coating-failure-scratch.pdf, accessed: 29.11.2020.

[33] S.T. Gonczy, N.X. Randall, *An ASTM Standard for Quantitative Scratch Adhesion Testing of Thin, Hard Ceramic Coatings*, International Journal of Applied Ceramic Technology, vol. 2, iss. 5, pp. 422-428, 2005, doi: 10.1111/j.1744-7402.2005.02043.x

[34] S.J. Bull, E. Berasategui, *An Overview Of The Potential Of Quantitative Coating Adhesion Measurement By Scratch Testing*, Tribology and Interface Engineering Series, vol. 51, pp. 136-165, 2006, doi: 10.1016/S0167-8922(06)80043-X

[35] M.F. Othman, A.R. Bushroa, W.N.R. Abdullah, *Evaluation techniques and improvements of adhesion strength for TiN coating in tool applications: a review*, Journal of Adhesion Science and Technology, vol. 29, iss 7, pp. 569-591, 2015, doi: 10.1080/01694243.2014.997379

[36] C. Ping-wei, W. Shao-ming, W. Feng-Hui, *Fracture Analysis of Thermal Barrier Coating Delamination under Thermal Shock*, Procedia Engineering, vol. 99, pp. 344-348, 2015 doi: 10.1016/j.proeng.2014.12.545

[37] T. Katagiri, Y. Yamasaki, A. Yoshitake, *Effects of tool coatings on galling prevention in forming of high strength steels*, in Proceedings of the International Conference on Tribology in Manufacturing Process, 26-26 September, 2007, Yokohama, Japan, pp. 41-46.

[38] P. Lu, X. Xiao, Y.K. Chou, *Interface delamination study of diamond-coated carbide tools considering coating fractures*, Surface and Coatings Technology, vol. 260, pp. 239-245. 2014, doi: 10.1016/j.surfcoat.2014.08.080

[39] P.L. Menezes, M. Nosonovsky, S.P. Ingole, S.V. Kailas, M.R. Lovell, *Tribology for Scientists and Engineers: From Basics to Advanced Concepts*, Springer, 2013.

[40] Y. Hou, Z. Yu, S. Li, *Galling failure analysis in sheet metal forming processes*, Journal of Shanghai, Jiaotong University, vol. 15, iss. 2, pp. 249-249, 2010, doi: 10.1007/s12204-010-8007-z

[41] M. Clapa, D. Batory, *Improving adhesion and wear resistance of carbon coatings using Ti:C gradient layers,* Journal of Achievements in Materials and Manufacturing Engineerig, vol. 20, iss. 1-2, pp. 415-418, 2007.

[42] L. Żukowska, J. Mikuła, M. Staszuk, M. Musztyfaga-Staszuk, *Structure and Properties Of PVD Coatings Deposited On Cermets*, Archives of Metallurgy and Materials, vol. 60, iss. 2, pp. 727-733, 2015, doi: 10.1515/amm-2015-0198

[43] H. Bai, L. Zhong, Z. Shang, Y. Xu, H. Wu, Y. Ding, *Microstructure and mechanical properties of TiC-Fe surface gradient coating on a pure titanium substrate prepared in situ*, Journal of Alloys and Compounds, vol. 771, pp. 406-417, 2019, doi: 10.1016/j.jallcom.2018.08.316

[44] L.A. Dobrzański, L.W. Żukowska, *Structure and properties of gradient PVD coatings deposited on the sintered tool materials*, Open Access Library, vol. 1, pp. 187-231, 2011

[45] N. Cameron, Z. Farhat, *Fabrication, Characterization, and Evaluation of Monolithic NiTi Nanolaminate Coatings*, Tribology Transactions, vol. 62, iss. 6, pp. 1007-1018, 2019, doi: 10.1080/10402004.2019.1640331

[46] Z.H. Xie, M. Hoffmann, P. Munroe, R. Singh, *Microstructural response of TiN monolithic and multilayer coatings during microscratch testing*, Journal of Materials Research, vol. 22, iss. 8, pp. 2312-2318, 2007, doi: 10.1557/jmr.2007.0292

[47] J. Shuai, X. Zuo, Z. Wang, P. Guo, B. Xu, J. Zhou, A. Wang, P. Ke, *Comparative study on crack resistance of TiAlN monolithic and Ti/TiAlN multilayer coatings,* Ceramics International, vol. 46, iss. 5, pp. 6672-6681, 2020, doi: 10.1016/j.ceramint.2019.11.155

[48] F. Petit, C. Ott, F. Cambier, *Multiple scratch tests and surface-related fatigue properties of monolithic ceramics and soda lime glass*, Journal of the European Ceramic Society, vol. 29, iss. 8, pp. 1299-1307, 2009, doi: 10.1016/j.jeurceramsoc.2008.09.019